

Reverse dark resonance in Rb excited by a diode laser

Janis Alnis and Marcis Auzinsh

Department of Physics, University of Latvia, 19 Rainis Boulevard, Riga, LV-1586, Latvia

Received 20 March 2001, in final form 20 July 2001

Published 5 October 2001

Online at stacks.iop.org/JPhysB/34/3889

Abstract

The origin of recently discovered reverse (opposite-sign) dark resonances has been explained theoretically and verified experimentally. It is shown that the reason for these resonances is a specific optical pumping of the ground state magnetic sublevel in a transition when the ground state angular momentum is smaller than the excited state momentum. An experiment was conducted on ^{85}Rb atoms in a cell, when a diode laser using the ground state hyperfine level $F_g = 3$ simultaneously excites spectrally unresolved hyperfine levels with total angular momentum quantum numbers $F_e = 2, 3$ and 4. It is shown that due to differences in the transition probabilities the dominant role in total absorption and fluorescence signals is played by absorption on a transition $F_g = 3 \rightarrow F_e = 4$.

1. Introduction

Coherent population trapping was discovered in the interaction of sodium atoms with a laser field in 1976 [1]. Due to this effect a substantial part of the population (because of destructive quantum interference between different excitation pathways) is trapped in a coherent superposition of the ground state sublevels, i.e. dark states. Dark resonances are associated with coherent population trapping. This means that, due to the population trapping in the ground state, laser light absorption and, as a result, fluorescence from an ensemble of atoms decreases, while simultaneously the intensity of the transmitted light increases. If in addition to the optical excitation an external magnetic field is applied perpendicular to the light polarization, it can destroy the coherence between the ground state sublevels and return the trapped population to the absorbing states and result in increasing absorption and fluorescence, and decreasing the transmitted light. Some years ago Arimondo published a review [2] of the applications of dark resonances.

Coherence in an atomic ground state recently attracted substantial attention in connection with lasing without inversion [3], magnetometry [4], laser cooling [5], electromagnetically induced transparency [6] and very recently in connection with coherent information storage using halted light pulses [7, 8]. As a result dark resonances have been studied in detail, including open systems [9] and systems with losses [10]. During these studies the authors

of [11] observed a new and unexpected phenomenon. In this study the D_2 line of ^{85}Rb atoms was excited by a diode laser. The radiation was tuned to the absorption from the optically resolved ground state hyperfine level $F_g = 3$ originating from atomic $5S_{1/2}$ state. The final state of the transition was the $\text{Rb } 5P_{3/2}$ excited state. Hyperfine components of this level were not resolved, and all dipole-allowed transitions to the excited state hyperfine levels with quantum numbers $F_e = 2, 3$ and 4 were excited simultaneously. At the same time one should note that although the hyperfine components of the excited state were not resolved within the Doppler linewidth, the laser linewidth was sufficiently narrow to excite different hyperfine transitions in different velocity classes of atoms. Consequently, each hyperfine transition under experimental conditions was excited almost independently from the other transitions despite the fact that all transitions had the same ground state level with quantum number $F_g = 3$.

In contrast to the usual dark resonance signal, the authors of [11] have observed the opposite effect—i.e. a decreased transmittance of laser radiation and increased fluorescence intensity was observed when the magnetic field was set to zero. The gas became more transparent and the fluorescence intensity decreased when the magnetic field was applied. According to the authors of [11] the physical reason for this effect *still remains unclear*.

In this paper we offer, in our opinion, a very simple and straightforward explanation of the origin of these ‘reverse’ dark resonances and carry out an experimental and numerical study.

2. Reverse resonance

In a simple qualitative explanation traditional dark resonances can be related to a well known optical pumping phenomenon. Let us assume that we excite an atomic transition $F_g = 2 \rightarrow F_e = 1$ with linearly polarized light. The direction of the z -axis is chosen to be along the light electric field vector \mathbf{E} . As a result π absorption takes place and transitions occur between the ground and excited state magnetic sublevels with $\Delta M = M_g - M_e = 0$, where M_g and M_e are magnetic quantum numbers of the ground and excited state, respectively (see figure 1). According to this scheme absorption does not take place from the ground state magnetic sublevels with quantum numbers $M_g = \pm 2$, because for these states there are no corresponding excited state magnetic sublevels with the same magnetic quantum number value.

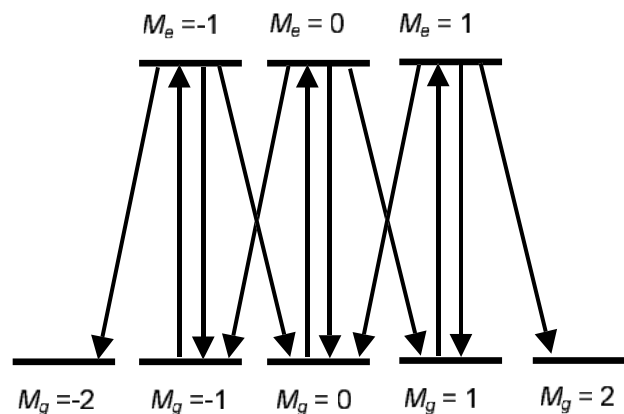


Figure 1. Allowed dipole transition scheme for ground state optical pumping in the case of π absorption for $F_g = 2 \rightarrow F_e = 1$.

In spontaneous decay, dipole transitions from optically populated excited state magnetic sublevels $M_e = \pm 1$ to the non-absorptive ground state sublevels $M_g = \pm 2$ are allowed. Consequently, if relaxation in the ground state is slow, under steady-state conditions a substantial part of the population will be optically pumped to the ground state sublevels with quantum numbers $M_g = \pm 2$ and will be trapped there. As a result the traditional decrease of the absorption and fluorescence, and increase of the transmittance will be observed, because the population of the absorbing ground state magnetic sublevels will be reduced.

If at that moment an external magnetic field is applied in a direction perpendicular to the z -axis (light polarization \mathbf{E}), the field will effectively mix the ground state sublevels and will return the trapped population into the states from which the absorption takes place. It will increase absorption and fluorescence. This is a qualitative explanation of the usual dark resonance.

Similar reasoning can be used to explain the ‘reverse’ resonance reported in [11] and in this paper. Let us assume that we excite with π radiation the atomic transition $F_g = 1 \rightarrow F_e = 2$. In this case all magnetic sublevels absorb light, and there are no sublevels that can trap the atomic population. Absorption rates between respective magnetic sublevels for linearly polarized π absorption may be calculated as

$$\Gamma_{M_g \rightarrow M_e} = \Gamma_p \frac{2F_g + 1}{2F_e + 1} (C_{F_e M_e}^{F_g M_g})^2 \quad (1)$$

where Γ_p denotes the absorption rate, but $C_{\alpha\alpha\beta\beta}^{CY}$ denotes the respective Clebsch–Gordan coefficients. The rates of the spontaneous transitions between the excited and ground state magnetic sublevels may be calculated as

$$\Gamma_{M_e \rightarrow M_g} = \Gamma \frac{2F_e + 1}{2F_g + 1} (C_{F_e M_e}^{F_g M_g})^2 \quad (2)$$

where Γ is the spontaneous relaxation rate of the excited state. Relative transition rates between magnetic sublevels of the $F_g = 1 \leftrightarrow F_e = 2$ transition, calculated according to formulae (1) and (2), are shown in figure 2. As one can see from this figure, the ground state magnetic sublevel $M_g = 0$ is the most absorbing one, with the highest relative absorption rate. At the same time, all three excited state magnetic sublevels populated by light absorption decay strongly just to this sublevel, with high rates. One can expect that in a situation of steady-state excitation, as a result of the interplay between the absorption and the decay rates, the

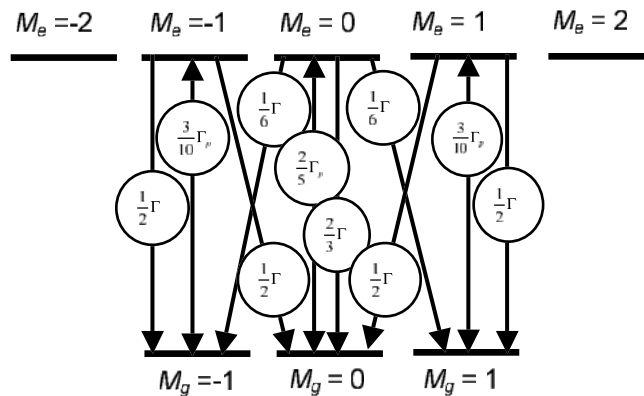


Figure 2. Transition scheme and rate constants for π absorption in the case of $F_g = 1 \rightarrow F_e = 2$.

population of the strongly absorbing ground state magnetic sublevel $M_g = 0$ will be increased and, consequently, one can expect increased absorption and fluorescence from this atom and decreased transmittance of the resonant laser light.

If an external magnetic field is applied perpendicular to the z -axis it will mix the ground state magnetic sublevels and redistribute the population between them. Consequently, the population of the strongly absorbing magnetic sublevel $M_g = 0$ will be decreased. At the same time, the population of less strongly absorbing magnetic sublevels $M_g = \pm 1$ will be increased. This means that the total absorption and fluorescence will be decreased and transmittance will be increased. As a result reverse dark resonance will be observed.

Let us solve the balance equations for the magnetic sublevel stationary population n_{M_g} in the scheme shown in figure 2 to prove this qualitative consideration. With the steady-state conditions for the ground state magnetic sublevels we obtain

$$\begin{aligned} n_{-1} &= \frac{6(10\Gamma + 3\Gamma_p)}{5(17\Gamma + 12\Gamma_p)} \bar{n}_g \\ n_0 &= \frac{27(5\Gamma + 2\Gamma_p)}{5(17\Gamma + 12\Gamma_p)} \bar{n}_g \\ n_{+1} &= \frac{6(10\Gamma + 3\Gamma_p)}{5(17\Gamma + 12\Gamma_p)} \bar{n}_g \end{aligned} \quad (3)$$

where \bar{n}_g is the ground state magnetic sublevel population in the absence of radiation. In the limit when absorption is slow $\Gamma_p \ll \Gamma$ (weak absorption), we have

$$\begin{aligned} n_{-1} &\approx \frac{12}{17} n_g \approx 0.706 \bar{n}_g \\ n_0 &\approx \frac{27}{17} n_g \approx 1.59 \bar{n}_g \\ n_{+1} &\approx \frac{12}{17} n_g \approx 0.706 \bar{n}_g. \end{aligned} \quad (4)$$

This type of optical pumping in a transition $F \rightarrow F + 1$ was briefly discussed for the first time in [12] and was analysed recently in [13, 14]. If we now bear in mind the absorption rates from different magnetic sublevels of the ground state (see figure 2), and calculate the overall absorption

$$I_a = \sum_{M_g=-F_g}^{F_g} \sum_{M_e=-F_e}^{F_e} n_{M_g} \cdot \Gamma_{M_g \rightarrow M_e} \quad (5)$$

from such a state and compare it with the absorption from the equally populated magnetic sublevels then we see an increase in the total absorption by a factor of $18/17 \approx 1.059$ or by approximately 5.9%.

The same calculation can be applied to the transitions $F_g = 2 \rightarrow F_e = 3$, $F_g = 3 \rightarrow F_e = 4$, $F_g = 4 \rightarrow F_e = 5$ and $F_g = 5 \rightarrow F_e = 6$. For these schemes we will similarly obtain an even larger increasing absorption caused by this specific optical pumping. The increase factor will be $540/461 \approx 1.17$, $4004/3217 \approx 1.24$, $119\,340/92\,377 \approx 1.29$ and $1790\,712/1352\,077 \approx 1.32$, respectively. This means that the described effect increases with increase of the quantum numbers of the involved levels and can reach remarkably large values.

The presented description is of course qualitative in the sense that it does not allow prediction of the form and width of the reverse dark resonance. In our opinion nevertheless it gives a good idea about what is happening when reverse dark resonances are observed. In order to have a quantitative description of the phenomenon one must solve the equations for the density matrix for an open system with losses.

3. Expected signal

We will use equations of motion for a density matrix to perform a more accurate numerical simulation of the expected reverse dark resonance signal. They are written under the assumption of a broad spectral line excitation [15]:

$$\begin{aligned} \dot{f}_{M_e M'_e} = & \Gamma_p \sum_{M_g M'_g} \langle M_e | \mathbf{E}^* \mathbf{d} | M_g \rangle \langle M'_e | \mathbf{E}^* \mathbf{d} | M'_g \rangle^* \varphi_{M_g M'_g} \\ & - \left(\frac{\Gamma_p}{2} + i\omega_S \right) \sum_{M''_e M_g} \langle M_e | \mathbf{E}^* \mathbf{d} | M_g \rangle \langle M''_e | \mathbf{E}^* \mathbf{d} | M_g \rangle^* f_{M''_e M'_e} \\ & - \left(\frac{\Gamma_p}{2} - i\omega_S \right) \sum_{M''_e M_g} \langle M''_e | \mathbf{E}^* \mathbf{d} | M_g \rangle \langle M_e | \mathbf{E}^* \mathbf{d} | M_g \rangle^* f_{M_e M''_e} \\ & - \Gamma f_{M_e M'_e} - i\omega_{M_e M'_e} f_{M_e M'_e} \end{aligned} \quad (6)$$

$$\begin{aligned} \dot{\varphi}_{M_g M'_g} = & - \left(\frac{\Gamma_p}{2} + i\omega_S \right) \sum_{M''_e M_e} \langle M_g | \mathbf{E}^* \mathbf{d} | M_e \rangle \langle M''_e | \mathbf{E}^* \mathbf{d} | M_e \rangle^* \varphi_{M''_e M'_g} \\ & - \left(\frac{\Gamma_p}{2} - i\omega_S \right) \sum_{M''_e M_e} \langle M''_e | \mathbf{E}^* \mathbf{d} | M_e \rangle \langle M_g | \mathbf{E}^* \mathbf{d} | M_e \rangle^* \varphi_{M_g M''_e} \\ & + \Gamma_p \sum_{M_e M'_e} \langle M_g | \mathbf{E}^* \mathbf{d} | M_e \rangle \langle M'_g | \mathbf{E}^* \mathbf{d} | M'_e \rangle^* f_{M_e M'_e} \\ & - \gamma \varphi_{M_g M'_g} - i\omega_{M_g M'_g} \varphi_{M_g M'_g} + \sum_{M_e M'_e} \Gamma_{M_g M'_g}^{M_e M'_e} f_{M_e M'_e} + \lambda \delta_{M_g M'_g} \end{aligned} \quad (7)$$

where $f_{M_e M'_e}$ and $\varphi_{M_g M'_g}$ denote density matrices of the excited and ground state level, respectively. The first term on the right-hand side of equation (6) describes the effect of light absorption on $f_{M_e M'_e}$ at an absorption rate Γ_p . The matrix elements of the form $\langle M_e | \mathbf{E}^* \mathbf{d} | M_g \rangle$ account for the conservation of the angular momentum in photon absorption, from the light wave with unit polarization vector \mathbf{E} . The second and third terms jointly describe the stimulated emission of light and the shift in the dynamic Stark effect by frequency ω_S . The fourth term characterizes the relaxation of the density matrix $f_{M_e M'_e}$ with a rate constant Γ . Finally, the fifth term on the right-hand side of equation (6) describes the effect of the external magnetic field, which produces splitting of the magnetic sublevels M_e and M'_e by a value of $\omega_{M_e M'_e} = (E_{M_e} - E_{M'_e})/\hbar$.

On the right-hand side of equation (7) the first and second terms jointly describe light absorption and the effect of the dynamic Stark effect. The third term describes stimulated light emission; the fourth term describes relaxation processes in the ground state and the fifth term describes the external magnetic field effect. The sixth term characterizes the reverse spontaneous transitions at a rate $\Gamma_{M_g M'_g}^{M_e M'_e}$, and finally, the seventh term describes the relaxation of the density matrix of the ground state atoms, interacting with the rest of the gas in a cell, which is not influenced by the excitation light.

In order to solve numerically the system of equations (6) and (7), the matrix element of the electric dipole transition $\langle M_e | \mathbf{E}^* \mathbf{d} | M_g \rangle$ may be expanded as

$$\langle M_e | \mathbf{E}^* \mathbf{d} | M_g \rangle = \sum_q (E^q)^* \langle M_e | d^q | M_g \rangle \quad (8)$$

where the superscript q denotes the cyclic components of the respective vectors. The remaining matrix element can be further expanded, by applying the Wigner–Eckart theorem,

$$\langle M_e | d^q | M_g \rangle = \frac{1}{\sqrt{2F_e + 1}} C_{F_g M_g 1 q}^{F_e M_e} (F_e \| d \| F_g) \quad (9)$$

where $(F_e \| d \| F_g)$ is the reduced matrix element. Under stationary excitation the system of equations (6) and (7) turn into a system of linear equations for the ground and excited state density matrix elements. The coefficients for this system of equations may be calculated by means of the angular momentum algebra and the formulae presented above.

For more details concerning the system of equations of motion for the density matrix in a broad excitation line limit and methods of solution, see [15].

The analysis of the probabilities [16]

$$W_{F_g \rightarrow F_e} = (2F_e + 1)(2F_g + 1)(2J_e + 1)(2J_g + 1) \begin{Bmatrix} J_g & F_g & I \\ F_e & J_e & 1 \end{Bmatrix}^2 \begin{Bmatrix} L_g & J_g & S \\ J_e & L_e & 1 \end{Bmatrix}^2 \quad (10)$$

of optical transitions, which originate from $F_g = 3$ for three excited state hyperfine levels of the ^{85}Rb atom, shows that the levels $F_e = 2, 3, 4$ are populated in the ratio $(5/18 \approx 0.278):(35/36 \approx 0.972):(9/4 = 2.25)$. This means that the absorption rates from the ground state hyperfine level to the respective excited state hyperfine level have the same ratio (see figure 3). For the D_2 line of the rubidium atom electronic angular momentum in the ground state is $J_g = \frac{1}{2}$, and for the excited state it is $J_e = \frac{3}{2}$. In the experiment, analysed here, the rubidium isotope ^{85}Rb was used, which has a nuclear spin of $I = \frac{5}{2}$.

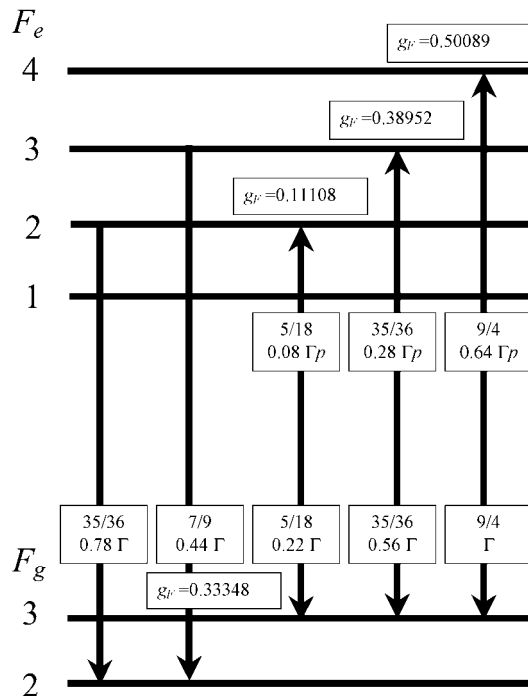


Figure 3. Relative transition strength and Landé factors of the hyperfine levels involved in formation of the reversed dark resonance signal in the ^{85}Rb atom.

In spontaneous emission there exists a disparity between the level $F_e = 4$ and all other excited state hyperfine levels involved in absorption. According to the selection rules for dipole transitions, the hyperfine level $F_e = 4$ can only decay to the initially absorbing level $F_g = 3$. This means that for this transition we have a closed cycle of optical pumping [17] with no losses. For all other excited state levels we have the possibility of spontaneously decaying to the initial level or to the other ground state hyperfine level $F_g = 2$. This decay constitutes the losses for an optical pumping. In this case the pumping cycle is open [17]. We can calculate the ratio between decay to the initial level $F_g = 3$ and the level $F_g = 2$ using the expression (10) again. We know that the total decay rate for the $5^2P_{3/2}$ state is $\Gamma = 3.8 \times 10^7 \text{ s}^{-1}$ [19]. The decay rates to both ground state hyperfine levels are shown in figure 3. We assume that the magnetic field used in the experiment, which is described and analysed below, is weak enough not to substantially mix the hyperfine levels. This means that the energies of magnetic sublevels M_e and M_g are linearly dependent on the magnetic field strength, and can be found as $E_{M_i} = g_{F_i} \mu_B M_i B$, where μ_B is the Bohr magneton and B denotes the magnetic field strength. The validity of these assumptions can be justified by the results of [18]. Landé factors g_{F_i} for each of the hyperfine levels can be calculated according to the well known method [20]. Numerical values of electronic and nuclear Landé factors for the Rb atom can be found in [21]. We have used the following values for $g_{5P_{3/2}} = 1.3362$, $g_{5S_{1/2}} = 2.00233$ and $g_I = -0.000293$. The rate equations (6) and (7) for a density matrix for all allowed transitions were solved numerically. Finally, the fluorescence signal for each transition was calculated according to [15]

$$I = \tilde{I}_o \sum_{M_e, M_g} \langle M_e | (\mathbf{E}')^* \mathbf{d} | M_g \rangle \langle M_e' | (\mathbf{E}')^* \mathbf{d} | M_g' \rangle^* f_{M_e' M_e} \quad (11)$$

where \mathbf{E}' is the polarization of the light, which we intend to observe and \tilde{I}_o is the coefficient of proportionality. Finally, the averaged total signal was calculated by taking into account the relative transition probabilities between different hyperfine levels, as shown in figure 3. The absorbed light intensity can be calculated by noting that the energy of the absorbed light is proportional to the total population created by this absorption in the excited state of atoms for each transition involved.

Initially for signal simulation we will analyse only the $F_g = 3 \rightarrow F_e = 4$ transition. The following rate constants were used in this simulation: the total absorption rate was assumed to be $\Gamma_p = 3 \times 10^6 \text{ s}^{-1}$; ground state relaxation rate $\gamma = 2 \times 10^5 \text{ s}^{-1}$ (mainly due to collisions with the walls of the cell and flight through [15] the excitation laser beam); excited state relaxation rate, $\Gamma = 3.8 \times 10^7 \text{ s}^{-1}$; Stark shift, $\omega_S = 0$. We presume that the magnetic field is applied along the z -axis. The laser light is linearly polarized along the y -axis. The intensity of the fluorescence with the same polarization as for excitation is calculated and the intensity of the transmitted beam is calculated. For this the excited state density matrix elements are obtained as solution of the system of equations (6) and (7). Then, knowing the excited state density matrix, the fluorescence intensity can be calculated according to equation (11). For the calculation of the absorbed light intensity we are using the fact that the total absorbed light intensity is proportional to the population of the excited state, which is created by the light absorption. It may be represented by a sum of diagonal elements of the excited state density matrix. For both signals the dependence on the applied external magnetic field was analysed. The results of signal simulations are presented in figure 4. They demonstrate well the pronounced reverse resonances and are in very good qualitative agreement with the measurements obtained in [11] (see figure 5 therein). Such a strong reverse resonance is caused by the fact that in the total signal the main contribution is from the $F_g = 3 \rightarrow F_e = 4$ transition. The reason for this is that according to the data presented above, $F_g = 3 \rightarrow F_e = 4$

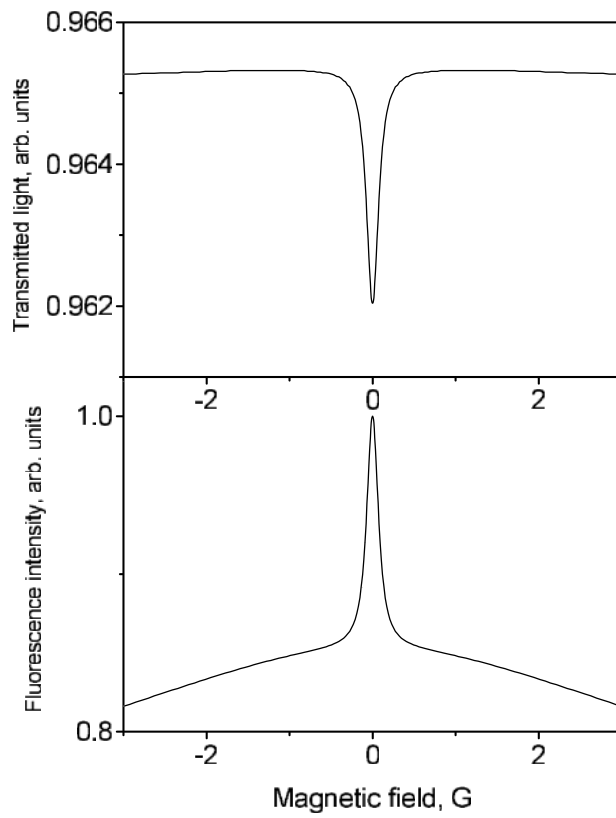


Figure 4. Calculated intensity of fluorescence and transmitted light for reverse dark resonance for $F_g = 3 \rightarrow F_e = 4$.

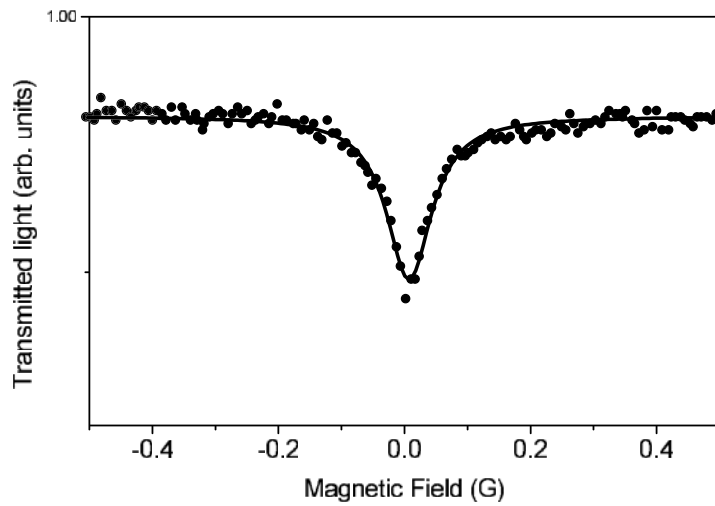


Figure 5. Measured (●) and simulated signal (full curve) for reverse dark resonance in ^{85}Rb .

is the strongest transition in the D_2 absorption. Besides, from the transitions involved in the laser light absorption, only the $F_g = 3 \rightarrow F_e = 4$ transition is a closed cycle transition. This means that only in this transition due to the selection rules do all excited atoms decay back to the initial level and the total number of atoms involved in an absorption–fluorescence cycle is conserved. In the other two transitions a certain number of the atoms decay to the other ground state hyperfine level $F_g = 2$, which do not absorb laser light with a given wavelength. As a result after several absorption–fluorescence cycles the number of atoms interacting with the laser light in these open-cycle transitions will be substantially reduced, and the absorption and fluorescence will be mainly determined by the $F_g = 3 \rightarrow F_e = 4$ transition. This effect should be well pronounced because, as already stressed, the laser line is sufficiently narrow spectrally to ensure that in each involved transition different velocity classes of atoms from the total ensemble interact with the laser. The width of the calculated resonances may be varied by changing the ground state Landé factor value, ground state relaxation rate and absorption rate.

In the weak absorption limit, $\Gamma_p \ll \Gamma$, the reverse dark resonance width is determined by a condition when the ground state Larmor frequency is equal to the ground state relaxation rate. For the $F_g = 3$ state of the ^{85}Rb atom at low concentration it can be as narrow as 20–30 mG. This is a width, which was actually observed in [11].

The obtained signals in some sense are the same as the ground state Hanle effect measured in atoms, as well as in molecules to a great extent (see, for example [15, 22]). In the case of molecules the reverse structure in the ground state Hanle effect was also observed. In the case of molecules, when optical pumping takes place in an open cycle and the total ground state population is substantially reduced due to intense absorption, this structure can be attributed to high-order coherence created by excitation light between distant ground state magnetic sublevels ($\Delta M = 6$ and greater) [23, 24]

4. Experimental

We have also carried out measurements of these reverse resonances in our laboratory. In our experiment we used isotopically enriched rubidium (99% ^{85}Rb) contained in a glass cell at room temperature to keep the atomic vapour concentration low and avoid reabsorption. The transition $5s^2S_{1/2} - 5p^2P_{3/2}$ at 780.2 nm is excited using both temperature- and current-stabilized single-mode diode lasers (Sony SLD114VS) with beam diameter 7 mm. The absorption signal (transmitted light) is monitored using a photodiode. As the laser frequency is swept by applying a ramp on the drive current, two absorption peaks with a half-width of about 600 MHz separated by about 3 GHz appear due to the ^{85}Rb ground state hyperfine structure. The excited state hyperfine structure is not resolved under the Doppler profile.

During the resonance measurements, the laser wavelength is stabilized on the absorption peak originating from the ground state hyperfine level $F_g = 3$.

Helmholz coils are used to sweep the magnetic field over the 0 G region. Additional coils compensate the Earth's magnetic field components.

The signal which is detected in transmitted light is averaged over 64 cycles and the result is presented in a figure 5 (data points and simulated signal). The amplitude of the experimental and calculated signals in arbitrary units and the curves in the figure are scaled so as to coincide at the minimum with the measured signal. For a simulated curve the parameters are chosen to have values that best reproduce our experimental conditions. The ground state relaxation rate $\gamma = v_p/r_0 = 0.07 \mu\text{s}^{-1}$ was chosen as a reciprocal time of thermal motion of Rb atoms at room temperature with the most probable velocity $v_p = 0.24 \text{ mm } \mu\text{s}^{-1}$ through the laser beam of radius $r_0 = 3.5 \text{ mm}$ [15]. The absorption rate was chosen as $\Gamma_p = 1.5 \mu\text{s}^{-1}$. Other

parameters are the same as in figure 4. Agreement between the calculated and the measured signal is remarkable and it seems to be possible to conclude that the proposed model explains the observed signal not only qualitatively but also quantitatively.

Acknowledgments

One of us (MA) is grateful to Professor Neil Shafer-Ray from the University of Oklahoma for fruitful discussions. Financial support from the Swedish Institute Visby programme is greatly acknowledged.

References

- [1] Alzetta G, Gozzini A, Moi L and Orrioli G 1976 *Nuovo Cimento B* **36** 5
- [2] Arimondo E 1996 *Prog. Opt.* **35** 257
- [3] Scully M, Zhu S-Y and Gavrielides A 1989 *Phys. Rev. Lett.* **62** 2813
- [4] Scully M and Fleischhauer M 1992 *Phys. Rev. Lett.* **69** 1360
- [5] Aspect A, Arimondo E, Kaiser R, Vansteenkiste N, Cohen-Tannoudji C 1988 *Phys. Rev. Lett.* **61** 826
- [6] Harris S 1997 *Physics Today* July 36
- [7] Philips D F, Fleischhauer A, Mair A, Walsworth R L and Lukin M D 2001 *Phys. Rev. Lett.* **86** 783
- [8] Liu C, Dutton Z, Behroozi C H and Hau L V 2001 *Nature* **409** 490
- [9] Ferruccio R, Albrecht L and Ennio A 1999 *Phys. Rev. A* **60** 450
- [10] Renzoni F, Maichen W, Windholz L and Arimondo E 1997 *Phys. Rev. A* **55** 3710
- [11] Dancheva Y, Alzetta G, Cartalava S, Taslakov M and Andreeva Ch 2000 *Opt. Commun.* **178** 103
- [12] Kazantsev A P, Smirnov V S, Tumaikin A M and Yagofarov I A 1984 *Opt. Spectrosk.* **57** 116
- [13] Renzoni F, Zimmermann C, Verkerk P and Arimondo E 2001 *J. Opt. B: Quantum Semiclass. Opt.* **3** S7
- [14] Renzoni F, Cartaleve S, Alzetta G and Arimondo E 2001 *Phys. Rev. A* **63** 065401
- [15] Auzinsh M and Ferber R 1995 *Optical Polarization of Molecules* (Cambridge: Cambridge University Press) p 305
- [16] Sobelman I I 1979 *Atomic Spectra and Radiative Transitions* (Berlin: Springer) p 359
- [17] Happer W 1972 *Rev. Mod. Phys.* **44** 169
- [18] Alnis J and Auzinsh M 2001 *Phys. Rev. A* **63** 023407
- [19] Belin G and Svanberg S 1971 *Phys. Scr.* **4** 269
- [20] Alexandrov E B, Chaika M P and Khvostenko G I 1993 *Interference of Atomic States* (New York: Springer) p 254
- [21] Arimondo E, Inguscio M and Violino P 1977 *Rev. Mod. Phys.* **49** 31
- [22] Auzinsh M P and Ferber R S 1991 *Phys. Rev. A* **43** 2374
- [23] Auzinsh M P and Ferber R S 1990 *Sov. Phys.-Usp.* **33** 833
- [24] Auzinsh M P and Ferber R S 1983 *Opt. Spectrosk.* **55** 674